

Numerical Determination of Inductance of a SMES Device Using the Response Surface Methodology Applied on FEM Modeling

Alin-Iulian Dolan and Florian Stefanescu

University of Craiova, Faculty of Electrical Engineering, Craiova, Romania, adolan@elth.ucv.ro, florian@elth.ucv.ro

Abstract — The paper proposes the determination of the inductance of a Superconducting Magnetic Energy Storage (SMES) device with modular toroid coil based on a new 2-D FEM modeling using the response surface methodology (RSM) applied on 3-D FEM modeling. An earlier 2-D FEM modeling of a SMES device created in FEMM software is based on the assumption of the equality between the inductances of the complete circular cross section toroid and of the rectangular cross section toroid, providing an approximation for the depth of planar model which does not take into account the leakage magnetic flux. Therefore a 3-D model of real geometry was realized using ANSYS software to improve this approximation. Imposing the equality of the magnetic field energies in 2-D and 3-D simulations, a new value for depth of 2-D FEM planar modeling is derived as polynomial regression of second order of the 3-D results, based on two factors characterizing the geometric torus shape: the coil inner diameter ratio and the coil thickness ratio. The application of analysis of variance (ANOVA) and the computation of some adjusting coefficients prove the descriptive and predictive power of this model. The inductances of different configurations of SMES device derived from the new 2-D FEM modeling are compared to those based on the earlier 2-D FEM modeling and on the 3-D FEM modeling. The results indicate an underestimation of the depth of the earlier 2-D FEM planar modeling and consequently, of the magnetic field energy and of the inductance for SMES devices with large inner diameter, when the leakage magnetic flux increases. The proposed model can improve the results of optimizations of the SMES device performed in previous papers.

Keywords—Inductance; SMES; FEM; DOE; RSM; ANOVA

I. INTRODUCTION

The design and the optimization of the Superconducting Magnetic Energy Storage (SMES) devices is a topic of permanent interest [1] - [8], many studies being developed during a research project [7].

The numerical simulations help to preview the best solutions with minimum costs. In [6] and [9] were created 2-D and 3-D numerical models of a 21 kJ modular toroid coil system, using finite element method (FEM) in FEMM and ANSYS software. The results shown that a 2-D model under well-chosen assumptions can be as accurate as a 3-D model of the real geometry, which is much more expensive in terms of work time and hardware resources.

In [8] was established a geometric criteria for presizing of toroidal coil for magnetic energy storage in order to optimize the storage capacity, choosing two geometric

parameters. Based on analytical calculation, correlations between different dimensions have been derived.

In [10] and [11] are done optimized solutions of modular toroid coil geometry of a 21 kJ SMES device using design of experiments (DOE) and FEM.

In [12] is proposed the improving of the earlier 2-D modeling used in [6] by using polynomial regression models of first degree for the depth of planar modeling. This is based on equivalence of magnetic field energies between 2-D and 3-D simulations, using the response surface methodology (RSM) applied on 3-D FEM modeling.

The preoccupations to find a best modeling have been carried out and this paper proposes a new 2-D modeling based on a regression polynomial model of second degree for the depth parameter.

In the first part are presented some basic concepts in RSM concerning the polynomial models, the ways of estimation of their coefficients and the technique of analysis of variance (ANOVA) with some adjusting coefficients as tools for testing of the validity of the models and for appreciating their quality.

In the second part is described the methodology of obtaining of the second order model for the depth of 2-D FEM planar modeling. Based on the new model, the inductance for different configurations of the SMES device is determined and compared to those based on the earlier 2-D FEM modeling and on the 3-D FEM modeling. The ANOVA is applied and some adjusting coefficients are computed for statistical tests.

II. RESPONSE SURFACE METHODOLOGY

A. Basic Concepts in RSM

The response surface methodology (RSM) is a useful technique for modeling and analysis of the response of a system influenced by a set of independent factors. The design of experiments (DOE) is essentially based on the creation and exploitation of the models of the response consisting of analytical relationship describing the variations of the response versus to the variation of the factors. [13] - [16].

Usually, the RSM problems use polynomial models of first- or second-order derived as results of a series of experiments with different values for the factors.

For a set of k factors, the model function (called regression) Y_{mod} approximates the value of response Y for any combination of the factors by matrix-form relationship

$$Y_{\text{mod}}(\mathbf{x}) = f(\mathbf{x}) \cdot \boldsymbol{\beta}, \quad (1)$$

where $\mathbf{x} = (x_1 \ x_2 \ \dots \ x_k)^T$ (2)

is the coordinates vector of an experience point P,

$$f(\mathbf{x}) = (1 \ x_1 \ \dots \ x_k \ x_1 x_2 \ \dots \ x_1 x_k \ \dots \ x_2 x_k \ \dots \ x_1^2 \ \dots \ x_k^2) \quad (3)$$

is a line vector whose elements contain the values of the k factors and theirs possible combinations by mutual multiplications up to second order and

$$\boldsymbol{\beta} = (b_0 \ b_1 \ \dots \ b_k \ b_{12} \ \dots \ b_{1k} \ \dots \ b_{2k} \ \dots \ b_{11} \ \dots \ b_{kk})^T \quad (4)$$

is the vector of the correspondents coefficients, with p elements.

1) *The first-order model without interactions* does not take into account the interaction between the factors. For two factors denoted $x_1 = x$ and $x_2 = y$, we have $p = 3$ and

$$\mathbf{x} = (x \ y)^T, \quad f(\mathbf{x}) = (1 \ x \ y), \quad \boldsymbol{\beta} = (b_0 \ b_1 \ b_2)^T. \quad (5)$$

The values of the model function can be also written as

$$Y_{\text{mod}}(\mathbf{x}) = b_0 + \mathbf{x}^T \cdot \mathbf{b}, \quad \mathbf{b} = (b_1 \ b_2)^T. \quad (6)$$

The coefficient b_0 is the value of model function in the origin point $(0 \ 0 \ \dots \ 0)^T$ and the vector \mathbf{b} indicates the direction of the greatest increase of the model function.

2) *The first-order model with interactions* takes into account the interactions between the factors. For two factors in this case $p = 4$ and

$$f(\mathbf{x}) = (1 \ x \ y \ xy), \quad \boldsymbol{\beta} = (b_0 \ b_1 \ b_2 \ b_{12})^T. \quad (7)$$

3) *Second-order models* make appear quadratic terms and $p = 6$

$$f(\mathbf{x}) = (1 \ x \ y \ xy \ x^2 \ y^2), \quad \boldsymbol{\beta} = (b_0 \ b_1 \ b_2 \ b_{12} \ b_{11} \ b_{22})^T. \quad (8)$$

The values of the model function are deduced from matrix form equation:

$$Y_{\text{mod}}(\mathbf{x}) = b_0 + \mathbf{x}^T \cdot \mathbf{b} + \mathbf{x}^T \cdot \mathbf{B} \cdot \mathbf{x} \quad (9)$$

where \mathbf{B} is a quadratic matrix whose diagonal elements are the coefficients of the two-power terms and the others elements correspond to the terms of interactions between the factors

$$\mathbf{B} = \begin{bmatrix} b_{11} & b_{12}/2 \\ b_{12}/2 & b_{22} \end{bmatrix} \quad (10)$$

This model is only used in the RSM and it requires a reasonable number of experiments for its calculation.

4) *Greater than two order models* imply an important number of experiments, an uncertain approximation and the difficulty to understand the model variations and to use the mathematical relationship.

B. Estimation of Coefficients of Polynomial Models

For a series of N experiments, the value of the model function in any experience point $P_i(\mathbf{x}_i) = P_i(x_i, y_i)$ is

$$Y_{\text{mod}}(\mathbf{x}_i) = f(\mathbf{x}_i) \cdot \boldsymbol{\beta}, \quad 1 \leq i \leq N. \quad (11)$$

The vectors \mathbf{Y} and \mathbf{Y}_{mod} bring together all the responses respectively their models and a new matrix form relationship can be written [13]

$$\mathbf{Y} = (\mathbf{Y}(\mathbf{x}_1) \ \dots \ \mathbf{Y}(\mathbf{x}_N))^T, \quad (12)$$

$$\mathbf{Y}_{\text{mod}} = (\mathbf{Y}_{\text{mod}}(\mathbf{x}_1) \ \dots \ \mathbf{Y}_{\text{mod}}(\mathbf{x}_N))^T = \mathbf{X} \cdot \boldsymbol{\beta}, \quad (13)$$

where $\mathbf{X} = (f(\mathbf{x}_1) \ \dots \ f(\mathbf{x}_N))^T$ (14)

is the design matrix built from the N experience points.

If $N = p$ experiences are performed, all the p coefficients can be uniquely determined by the system of linear equations

$$\mathbf{Y} = \mathbf{X} \cdot \boldsymbol{\beta}. \quad (15)$$

The model passes exactly through the experience points and the matrix \mathbf{X} is saturated (square).

If $N < p$, the above system is underdetermined, so one must always have $N \geq p$.

For the most common situations where $N > p$, the system (15) is overdetermined and there is enough information in the experimental data to estimate a unique value for $\boldsymbol{\beta}$ such that the model best fits the response. In this case the model cannot pass exactly through the experience points, but it commits an adjustment error in each of these points.

So there is an error vector $\boldsymbol{\varepsilon}$ (residue) nonzero. The coefficients must be estimated by the minimization a given criterion. The method of least squares is the best known and most used in the polynomial approximation.

The matrix-form relationship linking the response and the model function based on the estimation vector $\hat{\boldsymbol{\beta}}$ is

$$\mathbf{Y} = \mathbf{X} \cdot \hat{\boldsymbol{\beta}} + \boldsymbol{\varepsilon}. \quad (16)$$

The objective is the calculation of vector $\hat{\boldsymbol{\beta}}$ such that the vector $\boldsymbol{\varepsilon}$ to be minimized. The least squares criterion translates this requirement by an equivalent objective

$$\sum_{i=1}^N \varepsilon_i^2 = \sum_{i=1}^N (Y(\mathbf{x}_i) - Y_{\text{mod}}(\mathbf{x}_i))^2 \rightarrow \min \quad (17)$$

The estimation vector $\hat{\boldsymbol{\beta}}$ results

$$\hat{\boldsymbol{\beta}} = (\mathbf{X}^T \cdot \mathbf{X})^{-1} \cdot \mathbf{X}^T \cdot \mathbf{Y} \quad (18)$$

C. Analysis of Variance of the Model and Adjusting Coefficients

The ANOVA can be used to test the validity of the model function based on the relationship [13]

$$\mathbf{Y}^T \cdot \mathbf{Y} = \mathbf{Y}_{\text{mod}}^T \cdot \mathbf{Y}_{\text{mod}} + \boldsymbol{\varepsilon}^T \cdot \boldsymbol{\varepsilon}. \quad (19)$$

The left terms, called the total sum of the squares (SST), is composed of the sum of squares due to regression (SSR) and of the sum of errors squares (SSE), so

$$SST = SSR + SSE. \quad (20)$$

The variances (the mean squares) of the responses, regression and residues are deducted dividing the sums of squares by the corresponding degrees of freedom (DOF)

$$MST = \frac{SST}{N}, \quad MSR = \frac{SSR}{p}, \quad MSE = \frac{SSE}{N-p}. \quad (21)$$

In about all cases, the model contains a constant term which corresponds to coefficient b_0 , which is the average of responses

$$b_0 = \frac{1}{N} \sum_{i=1}^N Y(x_i) = \bar{Y}, \quad \bar{Y} = (\bar{Y} \dots \bar{Y})^T \quad (22)$$

Since this component is of no interest in ANOVA, it is usually suppressed. Consequently, the regression DOFs and total DOFs decrease by 1. Thus

$$MST_{-0} = \frac{SST}{N-1}, \quad MSR_{-0} = \frac{SSR}{p-1}. \quad (23)$$

Is then performed the Fisher-Snedecor test by calculating the ratio F_{obs} :

$$F_{\text{obs}} = \frac{MSR}{MSE} \quad \text{or} \quad F_{\text{obs}} = \frac{MSR_{-0}}{MSE_{-0}}. \quad (24)$$

The MSR (or MSR_{-0}) can be considered of the same order as the MSE (or MSE_{-0}) if the ratio F_{obs} is less than a statistical threshold. The null hypothesis H_0 means that $\beta = 0$. Under this assumption, F_{obs} is an observed value of a variable F of Fisher-Snedecor type, with p (or $p-1$) and $(N-p)$ DOFs. The hypothesis H_0 must be rejected at level λ when the probability $P(F \geq F_{\text{obs}}) \leq \lambda$.

The quality of a model can be evaluated by adjustments coefficients:

1) *Global variance of regression* ($\hat{\sigma}^2$) can be estimated by MSE . The model is the better fit to the experimental data as MSE is low

$$\hat{\sigma}^2 = MSE. \quad (25)$$

2) *Coefficient of determination* (R^2) is the ratio of the variance explained by the regression and the variance of responses, both corrected by the average value \bar{Y} .

$$R^2 = \frac{\mathbf{Y}_{\text{mod}}^T \cdot \mathbf{Y}_{\text{mod}} - \bar{Y}^T \cdot \bar{Y}}{\mathbf{Y}^T \cdot \mathbf{Y} - \bar{Y}^T \cdot \bar{Y}} = \frac{SSR_{-m}}{SST_{-m}} = \frac{SST_{-m} - SSE_{-m}}{SST_{-m}}. \quad (26)$$

This coefficient takes values between 0 and 1. A value close to 1 indicates a good model with a very good descriptive power.

3) *Adjusted coefficient of determination* (R_a^2) has the same signification as R^2 but it is defined in relation to corresponding DOFs

$$R_a^2 = \frac{\frac{SST_{-m}}{N-1} - \frac{SSE_{-m}}{N-p}}{SST_{-m}}. \quad (27)$$

It can take negative values if the R^2 is close to 0. Due to the consideration of DOFs one always has $R_a^2 < R^2$.

4) *Predictive Residual Sum of Square (PRESS)* is defined using the diagonal elements h_{ii} , $1 < i < N$, of the Hat matrix

$$\mathbf{H} = \mathbf{X} \cdot (\mathbf{X}^T \cdot \mathbf{X})^{-1} \cdot \mathbf{X}^T, \quad (28)$$

$$PRESS = \sum_{i=1}^N \frac{(Y(x_i) - Y_{\text{mod}}(x_i))^2}{(1 - h_{ii})^2}. \quad (29)$$

This coefficient is not a measure of adjustment, but rather an estimation of the predictive power of the model. It can be used to compare the models between them. One always has $PRESS \geq SSE$.

5) *Coefficient Q^2* is very similar to R^2 , often called "predictive R^2 "

$$Q^2 = \frac{SST_{-m} - PRESS}{SST_{-m}}. \quad (30)$$

It usually varies between 0 and 1. It can be negative for very poor models. The values close to 1 designates properly-fitting to experiments models.

The coefficients R^2 and Q^2 are thus two measures of goodness of fit: the first is an over-estimation while the second is an underestimation. R^2 is descriptive, measuring the relationship between the model function and the response in the initial experience points, while Q^2 is more predictive, measuring the ability of the model function to predict the response in unknown experience points.

6) *Distance of Cook* (δ)

In some cases, some values of the response may be aberrant even if their residues are not important. Therefore, it is better to review the influence of each experiment on the model function (coefficients). The distance Cook is defined as the distance between the estimation vector $\hat{\beta}$ and the estimation vector $\hat{\beta}_{(-i)}$ which do not take into account the i -th experiment

$$\delta_i = \frac{(\hat{\beta} - \hat{\beta}_{(-i)})^T \cdot (\mathbf{X}^T \cdot \mathbf{X}) \cdot (\hat{\beta} - \hat{\beta}_{(-i)})}{(p+1) \cdot MSE}. \quad (31)$$

The experiment i is considered of abnormal influences when their δ_i is greater than 1.

7) *Studentized residual* (t) is the quotient resulting from the division of a residual by an estimation of its standard deviation

$$t_i = \frac{Y(x_i) - Y_{\text{mod}}(x_i)}{\sqrt{MSE} \cdot \sqrt{1 - h_{ii}}}. \quad (32)$$

When N is large, the studentized residuals should be concentrated in the range $[-2; 2]$. High values may indicate abnormally high residuals.

The ANOVA and the adjustment coefficients allow evaluating the quality of the model. These tools require an additional cost of $(N-p)$ experiments compared to the calculation of a model requiring p experiments. There is therefore a compromise: possibility to evaluate the quality of the model or minimization of the effort for model calculation.

III. RSM APPLIED ON SMES DEVICE MODELING

A. SMES Geometry Description and Loads

The analyzed SMES device is shown in Fig. 1 [11]. For the shape of the coil, a modular toroid coil was chosen, consisting of solenoids connected in series and symmetrically arranged. This geometry can affect the size of SMES device, but the manufacturing process and feasibility are favored [2].

Each solenoidal coil is realized by NbTi superconductor (with Cu matrix) whose operating temperature is low (4.2 K), using liquid helium with all the implications of this extremely low temperature [4], [6], [8]. The specifications of such type of superconductor are presented in [3].

The basic dimensions are the mean diameter of modular toroid $D = 142$ mm, the coil inner diameter d and the coil thickness g . The number of solenoid modules is $n = 8$ and the cross section of the coil is $S = 128$ mm². According to specifications presented in [7], the radius of superconducting wire $r = 0.2$ mm and the thickness of carcass $p = 4$ mm.

The current density in superconductor was taken $j = 381.548$ MA/m², corresponding to a current $I = 75$ A. According to specifications presented in [5], the critical current density of NbTi superconductor at $T = 4.2$ K and $B_{lim} = 7$ T is $j_c = 530$ MA/m².

Two main parameters characterize the geometric torus shape: the coil inner diameter ratio α and the coil thickness ratio β .

They were chosen in [8] to optimize the storage capacity of a SMES device with toroidal coil

$$\alpha = \frac{d}{D}, \quad \beta = \frac{g}{D}. \quad (33)$$

The study domain is limited by a few constraints on position (Fig. 3).

$$\begin{cases} \alpha_{min} \leq \alpha \leq \alpha_{max} \\ \beta_{min} \leq \beta \leq \beta_{max} \\ g_{dist}(\alpha, \beta) \leq 0 \\ g_{diam}(\alpha, \beta) \leq 0 \end{cases}, \quad (34)$$

$$\text{where} \quad \alpha_{min} = 0.035 \leq \alpha \quad (35)$$

is in accord with manufacturing possibilities [7], (α_{max} , β_{min} and β_{max} are free),

$$g_{dist}(\alpha, \beta) = e_{min} - e(\alpha, \beta) \quad (36)$$

does not allow a distance e between two carcasses of solenoids less than $e_{min} = 5.425$ mm and

$$g_{diam}(\alpha, \beta) = E(\alpha, \beta) - D_{max} \quad (37)$$

that does not allow a total diameter of the modular toroid coil greater than $D_{max} = 230$ mm [7].

$$e(\alpha, \beta) = 2 \cdot \sin \frac{\varphi}{2} \cdot \left(r_0 - p - \frac{\frac{h}{2} + p}{\tan \frac{\varphi}{2}} \right), \quad (38)$$

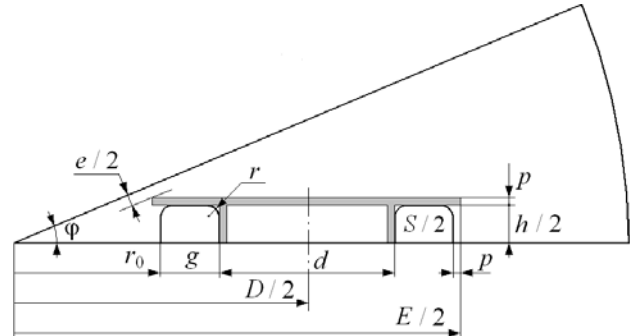


Fig. 1. Geometry of modular toroid coil [11].

$$r_0 = \frac{D-d}{2} - g = D \cdot \left(\frac{1-\alpha}{2} - \beta \right), \quad h = \frac{S}{g} = \frac{S}{\beta D}, \quad \varphi = \frac{2\pi}{n}, \quad (39)$$

$$E(\alpha, \beta) = D + d + 2g + p = D \cdot (1 + \alpha + 2\beta) + p. \quad (40)$$

B. Modeling of depth of 2-D Planar Model by RSM

The numerical simulations can be considered virtual experiments in which the studied object does not physically exist but its physical properties can be numerically calculated.

The virtual experiments are exempted from measurement errors being governed only by numerical errors (type of solving method, mesh characteristics, mathematical formulation and accuracy of numerical data).

The inductance L_c of the circular cross section toroid, with thin winding ($g \ll d, D$) (Fig. 2a), is [1]:

$$L_c = \frac{\mu_0}{2} \left[D - \sqrt{D^2 - d^2} \right]. \quad (41)$$

The earlier 2-D FEM model created in FEMM software describes a rectangular cross section toroid (Fig. 2b) [6], [9] whose inductance L_r can be calculated by [17]:

$$L_r = \frac{\mu_0}{2\pi} \cdot \text{depth} \cdot \ln \frac{D+d}{D-d}. \quad (42)$$

Under the assumption of the equality between the inductances of the complete circular cross section toroid L_c and of the rectangular cross section toroid L_r

$$L_c = L_r, \quad (43)$$

was derived the *depth* parameter describing the depth of the planar model. In a preliminary step of the research of SMES device [7], for $D = 300$ mm and $d = 0.15$ mm ($\alpha = 0.5$), it appears like a linear function of d

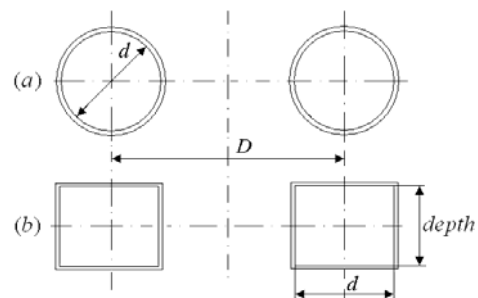


Fig. 2. Circular cross section toroid (a), rectangular cross section toroid (b).

$$depth = 0.766 \cdot d . \quad (44)$$

For $D = 142$ mm and a feasible range of d ($\alpha < 0.5$) the same relationship was used in 2-D FEM modeling, although an insignificant increase of the factor 0.766 can be observed with decreasing of ratio α .

The equivalence of the inductances does not take into account the leakage flux. Therefore a 3-D model of real geometry (Fig. 5) was realized using ANSYS software to improve the approximation (44).

Given the breadth of a 3-D simulation, reaching working times up to hours compared to working times of seconds order for a 2-D simulation, a new 2-D FEM modeling equivalent to 3-D modeling will be developed.

The magnetic field energy as result of 2-D simulation W_{m_2-D} is computed by multiplying the magnetic field energy per depth unity w_{m_2-D} by the parameter *depth*

$$W_{m_2-D} = w_{m_2-D} \cdot depth . \quad (45)$$

Imposing the equality of the magnetic field energies in 2-D and 3-D simulations, a new value *depth'* for depth of 2-D planar model can be derived

$$W_{m_3-D} = W'_{m_2-D} = w_{m_2-D} \cdot depth' = \frac{W_{m_2-D}}{depth} \cdot depth' , \quad (46)$$

$$depth' = \frac{W_{m_3-D} \cdot depth}{W_{m_2-D}} . \quad (47)$$

The inductance of SMES device can be evaluated by the relationship

$$L = \frac{2 \cdot W_{m_2D}}{I^2} . \quad (48)$$

It can be compared with the value done by 3-D FEM modeling, identical to the value done by 2-D FEM modeling, based on the new parameter *depth'*

$$L' = \frac{2 \cdot W_{m_3D}}{I^2} = \frac{2 \cdot W'_{m_2D}}{I^2} . \quad (49)$$

For each 3-D simulation, an equivalent 2-D simulation can be developed. To generalize the new 2-D FEM modeling for the ranges of factors α and β , a set of 3-D simulations are performed.

The runs on a PC with 1.5 MB RAM and 1.83 GHz processor frequency take more than 2 hours per simulation. Therefore, the number of the numerical experiments was limited to $N = 10$ for different levels of the factors α and β , adding a new one for testing of results.

The set of chosen experiments form a Simplex Lattice Design ($P_1 - P_6$) augmented with the axial points ($P_7 - P_{10}$) [14] for a better coverage of the study domain (Fig. 3).

Based on the results of 3-D simulations, a polynomial regression of second order is proposed for *depth* parameter depending on factors α and β :

$$depth''(\alpha, \beta) = b_0 + b_1\alpha + b_2\beta + b_{12}\alpha\beta + b_{11}\alpha^2 + b_{22}\beta^2 . \quad (50)$$

The estimation of the coefficients is made by the least squares criterion

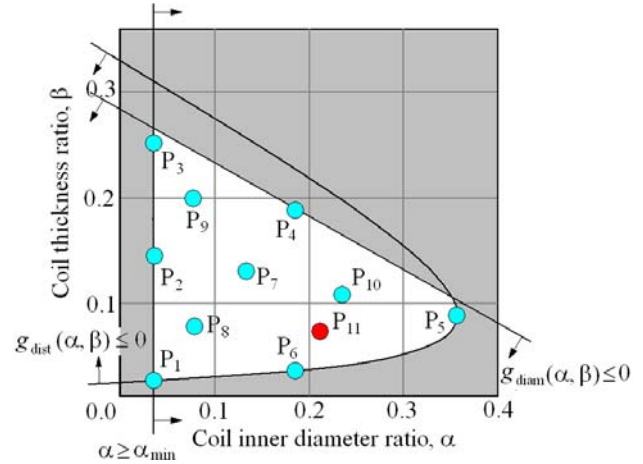


Fig. 3. Feasible domain defined by the constraints on position and the experience points (blue and red).

$$\sum_{i=1}^N (depth''(\alpha_i, \beta_i) - depth'(\alpha_i, \beta_i))^2 \rightarrow \min . \quad (51)$$

C. Numerical simulations

The perfect diamagnetism was simulated by considering the value of relative permeability of the superconductor close to zero [6]. The value $\mu_r = 10^{-7}$ is enough small for expulsion of magnetic field from superconducting domain (Fig. 4). Based on the symmetries, the sixteen-th part of the geometry was modeled to increasing the accuracy of the results. The mesh was realized using about 30000 nodes and 60000 triangular elements.

Commands files have been created using LUA scripting language. The zero tangential component of magnetic field strength was considered for the edges forming a

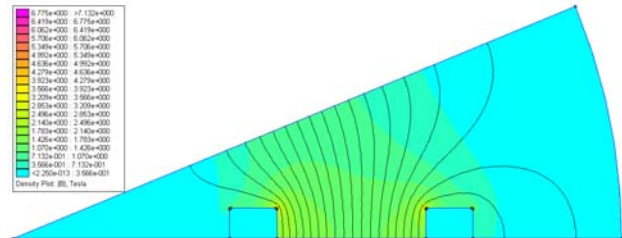


Fig. 4. Distribution of magnetic flux density for testing point P_{11} , 2-D FEMM, $\alpha = 0.22$, $\beta = 0.07$.

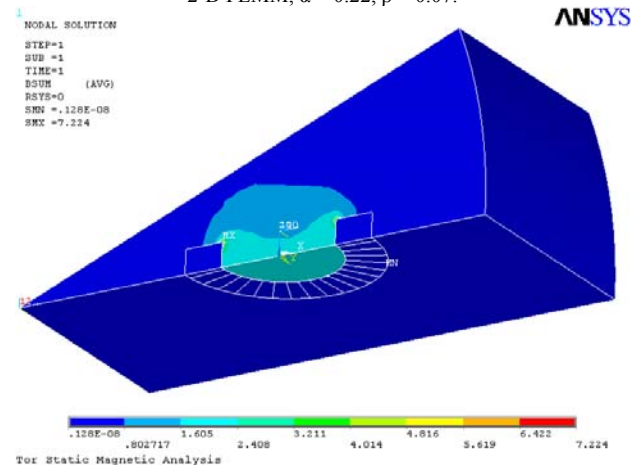


Fig. 5. Distribution of magnetic flux density for testing point P_{11} , 3-D ANSYS, $\alpha = 0.22$, $\beta = 0.07$.

sharp angle and zero magnetic vector potential, for the curve edge.

The MVP-edge based formulation has been employed for the analysis of static magnetic field of the 3-D coil, using the same simulated diamagnetism. Based on the symmetries, the thirty-two-th part of the geometry was modeled [9].

Commands files have been created using APDL (ANSYS Parameter Design Language). The mesh was realized using about 500000 nodes and 400000 tetrahedral elements, being limited by hardware resources. The flux normal conditions have been considered for the sides forming a sharp angle and the flux parallel conditions, for the others (Fig. 5).

IV. RESULTS AND CONCLUSIONS

The results of the $N = 10$ numerical experiments for parameter $depth'$ are presented in Table I adding a new one in postprocessing step (P_{11}), for testing of regression model.

The estimation of the vector of coefficients is

$$\hat{\beta} = \begin{pmatrix} -1.599 \\ 133.931 \\ 36.514 \\ 197.824 \\ -50.903 \\ -105.310 \end{pmatrix} \quad (52)$$

The results of ANOVA and the adjustment coefficients are presented in the Tables II–IV. The adjustment coefficients (Table II) show the descriptive and predictive power of the quadratic model.

The analysis of the distances of Cook (Table III) shows that about all the experiences have normal influences, excepting the point P_1 for which $\delta > 1$. The studentized residuals are normal, higher for the point P_4 .

The probability that the variance due to the regression will be significantly different from the residuals is 0.99999456 (Tables IV). The model can be considered of best quality, since there is more than 99% chance that they explain the variations in the responses.

In Fig. 6 is presented the quadratic regression for depth of 2-D FEM planar model compared to approximation (44) and to numerical experiments. It is found that the factor α has an important influence, as the (44) suggests. The model indicates a strong interaction between the factors, expecting significant variations in the directions α and β in the same time, so that using this model is justified.

For the lowest values of the factor α or of the factor β , the model agrees enough well with (44). The lowest values for α imply the invariance of depth parameter regardless the values of β . That means that the magnetic field energy and the inductance of devices of little inner diameter do not depend on the coil thickness.

In Table V are presented the values of the inductance done by old 2-D FEM model (L), by 3-D FEM model (L') and by new 2-D FEM model (L''). The relative errors related to 3-D results are computed resulting average errors of 30% for L , respectively, 3% for L'' .

TABLE I.
RESULTS OF 3-D NUMERICAL EXPERIMENTS

Experience points	α	β	$depth'$ [mm]
P_1	0.035000	0.024573	4.304607
P_2	0.035000	0.140000	6.332778
P_3	0.035000	0.250000	7.400906
P_4	0.196337	0.183522	32.354933
P_5	0.357674	0.087537	48.457262
P_6	0.196337	0.034660	24.789312
P_7	0.142558	0.125433	23.737578
P_8	0.088779	0.077000	13.320104
P_9	0.088779	0.187680	16.763830
P_{10}	0.250116	0.106485	36.884541
P_{11}	0.220000	0.070000	31.418055

TABLE II.
ADJUSTMENT COEFFICIENTS

R^2 [mm ²]	0.998883
R_a^2 [mm ²]	0.997491
$\hat{\sigma}$ [mm]	0.729933
$PRESS$ [mm ²]	34.774314
Q^2 [mm ²]	0.981802

TABLE III.
DISTANCES OF COOK AND STUDENTIZED RESIDUALS

Experience points	δ_i	t_i
P_1	3.389975	1.380130
P_2	0.647540	-1.611477
P_3	0.236433	0.424119
P_4	1.470154	-1.830231
P_5	0.330639	0.421181
P_6	1.329358	-1.408434
P_7	0.095457	1.318073
P_8	0.001477	-0.173564
P_9	0.020352	0.680271
P_{10}	0.005493	0.329613

TABLE IV.
RESULTS OF ANOVA FOR QUADRATIC REGRESSION

Source of variation	DOFs	SSR, SSE, SST [mm ²]	MSR, MSE, MST [mm ²]	F_{obs}
Regression	6-1=5	1908.710	381.742	716.479
Residual	10-6=4	2.131	0.533	Probability
Total	10-1=9	1910.844	212.316	0.99999456

TABLE V.
INDUCTANCES IN OLD AND IN NEW 2-D FEM MODELS AND IN 3-D MODEL AND RELATIVE ERRORS RELATED TO 3-D FEM MODEL

Exp. pts.	L [mH]	L' [mH]	L'' [mH]	$\frac{L-L'}{L'} \cdot 100\%$	$\frac{L''-L'}{L'} \cdot 100\%$
P_1	1.803	2.038	1.908	-11.56	-6.38
P_2	4.804	7.992	8.888	-39.88	11.22
P_3	5.685	11.051	10.906	-48.56	-1.31
P_4	75.893	114.980	117.332	-34.00	2.05
P_5	199.497	248.480	248.062	-19.71	-0.17
P_6	54.526	63.292	64.391	-13.85	1.74
P_7	43.054	65.908	63.638	-34.68	-3.45
P_8	18.621	25.685	25.896	-27.50	0.82
P_9	21.727	37.718	36.741	-42.40	-2.59
P_{10}	107.595	145.874	145.056	-26.24	-0.56
P_{11}	80.583	105.799	102.669	-23.83	-2.96

This 3% translates in fact the 3-D numerical errors. The 11-th 3-D simulation validates the quadratic regression, committing an error less than 3%.

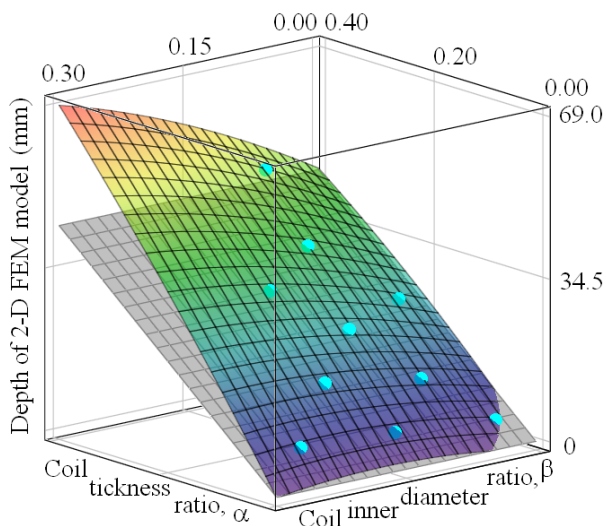


Fig. 6. Depth of 2-D FEM model: $depth$ (gray), $depth'$ (blue points) and $depth''$ (rainbow).

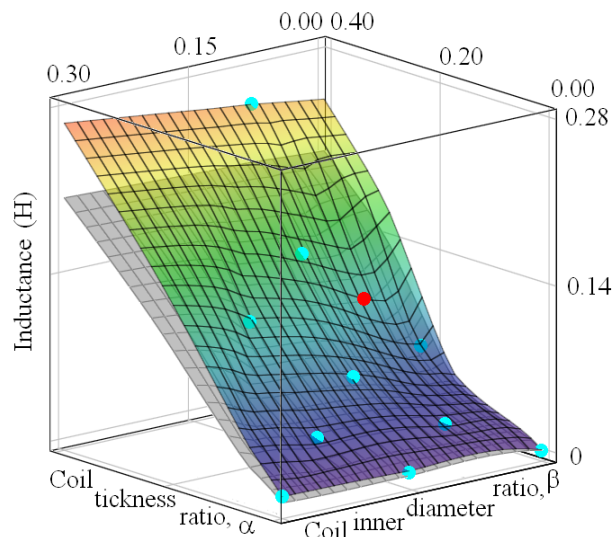


Fig. 7. Inductance: L (gray), L' (experience points P_1 - P_{10} - blue, testing point P_{11} - red) and L'' (rainbow).

The Fig. 7 illustrates the comparison of three values of the inductance for feasible ranges of factors α and β .

The new 2-D FEM model indicates an underestimation of the depth of the earlier 2-D planar modeling and consequently, of the magnetic field energy and of the inductance for devices with large inner diameter, when the leakage flux increases. The proposed model can improve the results of optimizations of the SMES device performed in [10], [11].

Received on July 15, 2015

Editorial Approval on November 24, 2015

REFERENCES

- [1] Floch, A. Lacaze, Y. Laumond, J. M. Kauffmann and P. Hiebel, "Dimensionnement et réalisation d'un SMES impulsional de 500J," *Eur. Physical Journal Applied Physics*, vol. 2, no. 1, pp. 17-25, 1998.
- [2] R. L. Causley, C. Cook and S. A. Gower, "Design of a high temperature superconductor magnetic energy storage system," *Proceedings of the Australasian Universities Power Engineering Conference (AUPEC-2001) - Perth*, September 23 - 26, pp. 322-325, 2001.
- [3] S. Nomura, H. Tsutsui, S. Tsuji-Iio, H. Chikaraishi and R. Shimada, "Feasibility study on high field magnets using stress-minimized helical coils," *Proceedings of the Fifteenth International Toki Conference on "Fusion and Advanced Technology"*, vol. 81, no. 20-22, pp. 2535-2539, 2006.
- [4] P. Tixador, "Superconducting magnetic energy storage: Status and perspective," *IEEE/CSC & ESAS European Superconductivity News Forum*, no. 3, January 2008.
- [5] F. Stefanescu, "Systemes de Stokage de l'energy electrique," 9th International Conference on Applied and Theoretical Electricity and 11th Symposium on Cryoelectrotechnics and Cryogenics, Craiova, October, 08-10, 2008, *Annals of the University of Craiova, Series: Electrical Engineering*, no.32, pp. 337-341, 2008.
- [6] F. Stefanescu and A. I. Dolan, "Conceptual design of 21 kJ superconducting magnetic energy storage device," *Annals of the Univ. of Craiova, Series: El. Eng.*, no. 34, pp. 109-112, 2010.
- [7] F. Stefanescu, "Technical and scientific report," 4-th part of Project "Sistem supraconductor pentru stocarea energiei electrice sub formă magnetică," PNCDI II 22113, Univ. of Craiova, 2011.
- [8] F. Stefanescu, "Geometry optimization of SMES coil," *Annals of the Univ. of Craiova, Series: El. Eng.*, no. 35, pp. 214-218, 2011.
- [9] A. I. Dolan and F. Stefanescu, "Three Dimensional Numerical Solution for Maximum Magnetic Field of 21 kJ Superconducting Magnetic Energy Storage Device," *Annals of the University of Craiova, Series: Electrical Engineering*, No. 37, pp. 73-77, 2013.
- [10] A. I. Dolan and F. Stefanescu, "Optimization of Modular Toroid Coil Geometry of a Superconducting Magnetic Energy Storage Device Using Design of Experiments and FEM," 12-th International Conference on Applied and Theoretical Electricity - ICATE 2014, Craiova, October 23-25, 2014.
- [11] A. I. Dolan and F. Stefanescu, "Application of two direct optimization methods on a SMES device by DOE and FEM: method by zooms and method by slidings of plans," *Annals of the University of Craiova, Series: El. Engineering*, No. 38, pp. 78-85, 2014.
- [12] A. I. Dolan and F. Stefanescu, "Improving of 2-D FEM Modeling of a SMES Device Using the Response Surface Methodology Applied on 3-D FEM Modeling," 10-th International Conference and Exhibition on Electromechanical and Power Systems - SIELMEN 2015 (in press).
- [13] S. Vivier, "Strategies d'optimisation par la methode des plans d'experiences et applications aux dispositives electrotechniques modelise par elements finis," Ph-D Thesis, Lille, 2002.
- [14] D. Montgomery, "Design and Analysis of Experiment," 5-th Edition, Arizona State University, 2000.
- [15] F. Gillon, "Modelisation et optimisation par plans d'experiences d'un moteur a commutations electronique," Ph-D Thesis, Lille, 1997.
- [16] M. Caldora-Costa, "Optimisation de dispositifs electromagnetiques dans un contexte d'analyse par la methode des elements finis," Ph-D Thesis, Grenoble, 2001.
- [17] F. E. Terman, "Radio Engineer's Handbook", McGraw-Hill, New York, 1943.